Experimental Evaluation of Frequency Regulation From Commercial Building HVAC Systems

Yashen Lin, Prabir Barooah, *Member, IEEE,* Sean Meyn, *Fellow, IEEE,* and Timothy Middelkoop

***Abstract*—Automated demand response can be a valuable resource for ancillary services in the power grid. This paper illustrates this value with the first experimental demonstration of frequency regulation from commercial building heating ventilation and air conditioning (HVAC) systems. The experiments were conducted in Pugh Hall, a 40 000 sq. ft. commercial building located at the University of Florida. Detailed are the steps required to make this possible, including control architecture, system identification, and control design. Experiments demonstrate: that satisfactory frequency regulation service can be provided by the HVAC system without noticeable effect on the indoor climate, and the ancillary service provided by this system passes the qualification criteria for participating in the Pennsylvania-New Jersey-Maryland (PJM) interconnection's frequency regulation market.**

***Index Terms*—Ancillary service, commercial buildings, frequency regulation, heating ventilation and air conditioning (HVAC) system.**

I. Introduction

Ancillary services are needed to correct the mismatch between demand and supply in a power grid. As more renewable energy sources are introduced into a power grid, the volatility of supply also increases, resulting in the need for additional ancillary services [1]. Ancillary services can be broadly divided into two categories: 1) those used continuously during normal operation; and 2) those used in contingency situations, such as following the loss of a generator. This paper focuses on frequency regulation, which falls in the first category. Frequency regulation corrects the short-term imbalance in the grid, usually on time scales of seconds to minutes [2]. The need for this service is well recognized based on engineering considerations, and consequently this is one of the ancillary services with a well developed market to incentivize service. The federal energy regulatory commission (FERC) has recognized the need for increasing ancillary services through several new rulings, such as the recent FERC order 755 [3] that demands payment for ancillary services in higher frequency bands.

Traditionally, frequency regulation has been provided by responsive power generators. Generators must withhold power to provide these services, and there is additional cost to generators in terms of both fuel and maintenance. Ramping of generation output also has cost in the form of additional pollution [4]. Finally, it is costly to build new generators to satisfy the increasing demand for ancillary services.

Recent research have shown that the demand side is capable of providing abundant high quality ancillary services, see [5]–[7]. Buildings are a tremendous untapped resource for several reasons. First, they are large energy consumers, accounting for 74% of total electricity consumption in the U.S. [8]. Residential loads, such as air conditioners and pool pumps, can be aggregated to provide ancillary service; see [9]–[12]. Manufacturing companies such as Alcoa Inc., provide demand side ancillary services today in a range of time scales [13].

We believe that heating ventilation and air conditioning (HVAC) systems in commercial buildings have significant potential for ancillary services that can be harnessed easily. Consumption of energy is very flexible, in part because of the large thermal inertia of the building. The power consumption of many commercial building HVAC systems can be varied continuously, which provides greater flexibility in control compared to on–off control commonly used in residential air conditioners. Commercial buildings are usually equipped with building automation system (BAS), which simplifies the installation of new control algorithms.

Simulations in [14] shows that continuous adjustment of the supply air fan in the air handling unit (AHU) in a commercial building can be used to provide frequency regulation in the frequency range of $f \in [1/(3 \text{ min}),\ 1/(8 \text{ s})]$, with negligible impact on room climate. If the chillers in the HVAC system are used, then the frequency range of ancillary service can be extended to low frequencies, down to $1/(1 \text{ h})$ [15].

All of this previous work was based on theory and simulations. To the best of our knowledge, this paper is the first to report implementation of HVAC control in a real building to provide frequency regulation. The field experiments are carried out in Pugh Hall, a building in the University of Florida campus that has a variable air volume (VAV) HVAC system.

The experiments reported here demonstrate that a building HVAC system can provide frequency regulation service inexpensively without affecting its primary

Manuscript received March 11, 2014; revised July 23, 2014 and September 25, 2014; accepted November 16, 2014. Date of publication January 1, 2015; date of current version February 16, 2015. This work was supported in part by the National Science Foundation under Grant CPS-0931416 and Grant ECCS-0925534, and in part by the U.S. Department of Energy Awards under Grant DE-OE0000097 and Grant DE-SC0003879. Paper no. TSG-00232-2014.

Y. Lin and P. Barooah are with the Mechanical and Aerospace Engineering Department, University of Florida, Gainesville, FL 32611 USA (e-mail: linyashen@gmail.com).

S. Meyn is with the Electrical and Computer Engineering Department, University of Florida, Gainesville, FL 32611-6130 USA.

T. Middelkoop is with the Industrial and Manufacturing Systems Engineering Department, University of Missouri, Columbia, MO 65211 USA.

Color versions of one or more of the figures in this paper are available online at http://ieeexplore.ieee.org.

Digital Object Identifier 10.1109/TSG.2014.2381596

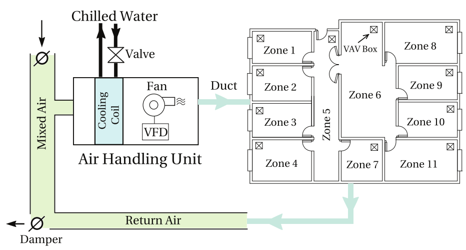

Fig. 1. Typical commercial building VAV HVAC system.

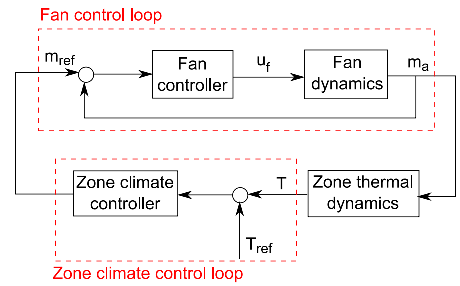

Fig. 2. Control loops in the AHU relevant to this paper. The zone climate control loop determines the desired supply air flow rate to maintain room temperature. The fan control loop commands the fan to produce that flow rate.

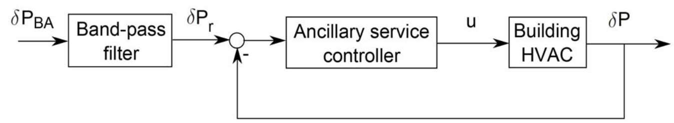

Fig. 3. Proposed control architecture.

responsibility—maintaining comfortable indoor climate. The control algorithms are tested with filtered regulation signals obtained from Pennsylvania-New Jersey-Maryland (PJM): the area control error (ACE) signal as well as the RegD signal [17]. Results show that the controllers introduced here have satisfactory performance in the frequency range of $f \in [1/(10\ \text{min}),\ 1/(30\ \text{s})]$, and will pass the PJM qualifying test [17].

This paper is inspired by our prior, simulation-based, studies on using HVAC fans to provide frequency regulation [7], [14], [16]. The control architectures used here are, however, quite distinct from those in our prior work. We demonstrate two distinct feedback control architectures to extract ancillary service by varying fan power consumption at distinct frequency bands. In one, the fan speed is commanded directly, while in the other it is varied indirectly through changing the air flow-rate setpoint. Each control design is based on black-box transfer functions obtained through system identification experiments.

Based on these experimental results, we estimate the economic value of building used in these experiments if it were to take part in PJMs ancillary service market, and the total amount of ancillary service that similar commercial buildings in the U.S. can provide through software retrofit.

The rest of this paper is organized as follows. In Section II, we briefly describe typical HVAC systems in commercial buildings and the proposed control architecture. The testbed where the experiments are conducted is described in Section III. In Section IV, models of HVAC system are identified experimentally for controller design and analysis, which is discussed in Section V. Experimental results are provided in Section VI. Section VII concludes this paper.

II. Problem Formulation

The control architecture described in this section is a software add-on for an existing HVAC control system. We first briefly review typical HVAC systems before describing this control architecture.

A. Typical HVAC System in Commercial Building

Fig. 1 shows the schematic of a VAV HVAC system; 30% of U.S. commercial building floorspace is serviced by such systems [18]. A part of return air is mixed with outdoor air, which is cooled and dehumidified while it passes through the cooling coil in the AHU. The air is distributed to terminal devices, called VAV boxes, through ducts for distribution into individual zones. A supply air fan motor in the AHU provides the mechanical energy required to circulate the air.

Highlighted in Fig. 2 are a few of many control loops in a HVAC system. The fan control loop and zone climate control loop are emphasized since they will be a focus of this paper. The zone climate controller compares the measured zone temperature T to a predetermined setpoint T_{ref} to compute a desired supply air flow rate m_{ref} to achieve the desired zone climate. The fan controller computes the fan command u_f to ensure that the supply air flow rate m_a tracks m_{ref}. In a VAV system, the fan motor speed is varied through a variable speed drive (VSD), so the command u_f is sent to the VSD. The fan command u_f is measured in the unit of percentage of the maximum speed.

B. Proposed Control Architecture

The goal of the control architecture described here is to provide ancillary service to the grid while ensuring that its actions have little effect on the indoor climate of the building. In this paper, we assume that a building HVAC system that provides frequency regulation service receives a signal from a balancing authority (BA), denoted by δP_{BA}, which is then filtered with a bandpass filter to generate a local reference signal, δP_r, which has the unit of power (W). Fig. 3 illustrates the proposed control architecture. The controller's responsibility is to vary the HVAC system's power consumption so that the deviation from baseline tracks the reference signal δP_r. The baseline power is the power the HVAC system would have consumed if it were only maintaining indoor climate under identical conditions, not providing ancillary service.

The design problem considered in this paper involves the ancillary service controller (ASC), which is local to the building. This controller addresses a reference tracking problem: commands to the AHU fan are modified in real-time so that δP, the deviation from the baseline power, tracks the reference deviation δP_r. Algorithms to estimate the deviation from baseline in real-time are described at the end of this section.

Recall that the primary functionality of the load must not be compromised in extracting ancillary services. Variations in

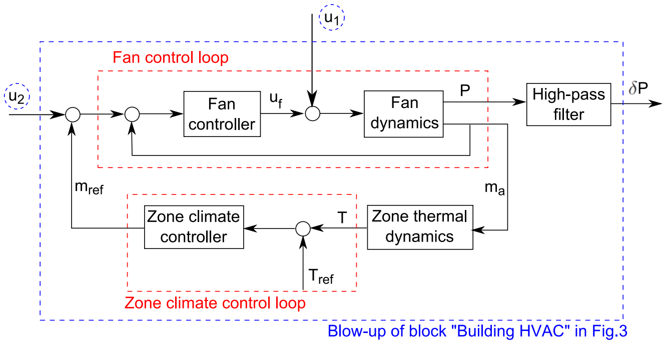

Fig. 4. Two locations to inject control command in the local control loop.

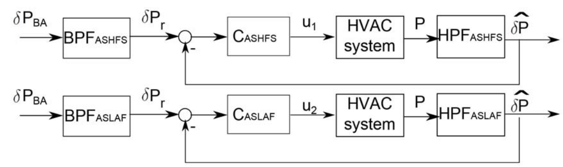

Fig. 5. Two control architectures resulting from the choice of actuation.

the airflow rate introduced by the ASC may change the indoor climate, which is undesirable. Moreover, the existing climate control system may negate the effect of the ASCs command, since the latter appears as a disturbance to the climate control system.

Ancillary service can be provided without running into these issues if the reference signal δP_r is chosen to be of sufficiently high frequency and sufficiently small amplitude. In particular, the frequency should be higher than the bandwidth of both the inner control loops (such as fan speed controller) and the bandwidth of the building's thermal response. Such frequency separation, together with a small amplitude in δP_r, would ensure that the response due to the disturbance δP_r at all the relevant outputs, such as fan speed, airflow rate, and indoor temperature would be small enough such that the building's preexisting control system would not reject the disturbance. In addition, small amplitude of δP_r will keep the variation in fan speed or airflow rate small, which will prevent adversely affecting equipment life and violation of ventilation requirements [19].

The passband frequencies and gains of the bandpass filter that filters δP_{BA} to produce the local reference signal δP_r have to be designed to satisfy these constraints. Due to the constraint that indoor climate should not be affected, the proposed architecture is suitable for high-frequency ancillary services such as frequency regulation, but may not be suitable for low-frequency ancillary services such as load following.

The passband of the bandpass filter and its passband gain will vary from building-to-building, depending on the capacity of its HVAC equipment, its thermal inertia, the bandwidth of the climate control loop, etc. In this paper, we assume that each building is free to design its own bandpass filter to ensure that its equipment is not damaged and its indoor climate is not adversely affected by the ancillary service it provides. Information on the filters is provided to the BA ahead of time, just like capacity bids by generators are provided today to ISOs so that the ISOs can determine if and when they have enough ancillary service resources.

The control signal u in Fig. 3 could be any command that changes the fan motor's power consumption. In this paper, we will explore two options, indicated as u_1 and u_2 in Fig. 4.

Utilization of the input u_1 is adopted from [14]: the ASC simply modifies the fan speed command u_f. In effect, the control command enters the existing HVAC control system as a disturbance (ignoring the feedback effect). Since the fan motor has fast dynamics, it can react quickly to track a high frequency reference signal. Low frequency variations of u_1 are not effective, since the local fan controller will reject the ancillary service control command as a disturbance.

The second option u_2 is a deviation to the baseline supply air flow rate m_{ref}. A change in the flow rate will result in a change in the fan motor power consumption. The zone climate control loop is usually less aggressive than the fan control loop, and is therefore likely to let lower frequency content in u_2 pass through without attenuation.

We will call the first option ASC for high frequency reference signal through fan speed command (ASHFS) and the second option ASC for low frequency reference signal through air flow setpoint (ASLAF). These are shown in Fig. 5. In principle, both controllers can be used simultaneously, though in the experiments and simulations reported here we use only one at a time.

The ASC described here is implemented as a software add-on to the existing climate control system; details are provided in Section III. As a result, the ASC does not override the existing HVAC control system, it merely modifies the commands in the HVAC system.

The deviation δP cannot be directly measured; only the power measurement P is available from the VSD. To obtain δP, we take advantage of the fact that reference signal has higher frequency than the dynamics of building HVAC system. The baseline power can be estimated on-line by passing P through a low-pass filter. The deviation from baseline, δP, can then be estimated by subtracting the estimated baseline from P. This is equivalent to using a high-pass filter; see Fig. 4. We denote this estimated power deviation by $\delta \hat{P}$.

III. Test Bed

The field experiments are carried out in 40 000 ft^2 building on the University of Florida campus, Pugh Hall. It has a VAV HVAC system and 3 AHUs. We choose AHU2, which is dedicated to a single auditorium, for conducting the tests. Fig. 6 shows data from a 24-h period during normal operation collected from AHU2 of Pugh Hall. The AHU is shut down from 11 P.M. to 6 A.M. every day. Even when the AHU is on and the climate control system is active (6 A.M.–11 P.M.), the space temperature varies by several °F, so any change smaller than that due to the ASC is unlikely to be noticed by the occupants.

Although Pugh Hall is equipped with a BAS (Siemens' APOGEE system), the BAS is not convenient for executing third party control algorithms in the building's equipment. A custom software was used to read values from and write

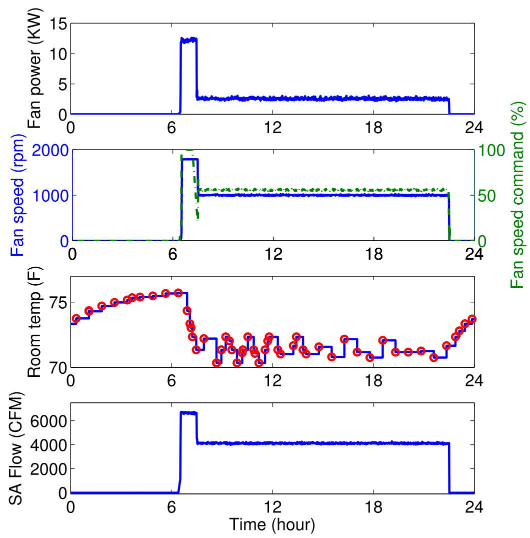

Fig. 6. Typical data from AHU2 in Pugh Hall during baseline operation.

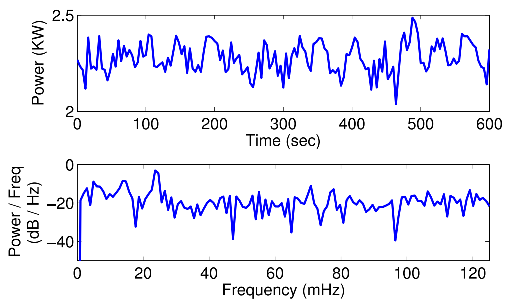

Fig. 7. Measurement noise characterization. Top: time domain power measurement. Bottom: power spectrum density of the noise.

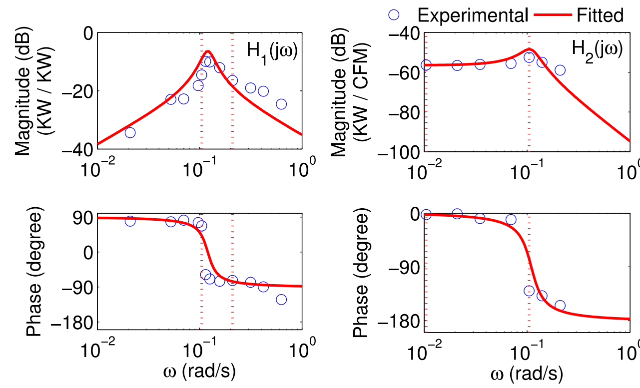

Fig. 8. Frequency response of H_1 (left) and H_2 (right) identified from sine-sweep experiments, as well as the bode plots of the fitted transfer functions.

commands to the HVAC equipment. The software is designed to simultaneously support a number of applications by interacting with various databases. Control commands from the applications are communicated to the software by appending a row to a table in a relational database. A scheduler, which checks for such updates every second, then communicates these new commands to the HVAC equipment through BACnet [20]. Partial details of the software are described in [21].

This software executes control commands during experiments by modifying commands from the building's climate control system without replacing the climate control system. For instance, during the experiments in which u_1 was used as the actuation, the command to the fan VSD computed by the fan controller was read, the value of u_1 computed by the ASC (or by the system identification algorithm) was added to it, and the sum was sent to the fan VSD through the software. A similar modification was done when u_2 was used as the actuation signal.

A. Measurement Noise

It was found that measurement noise is not negligible. Fig. 7 shows power measurements obtained over 10 min while the fan speed control command was set to a constant value of 55%. Also shown is an estimate of the power spectral density, which is consistent with white noise. The noise affects the estimate in system identification and the performance of the controllers, which will be discussed in later sections.

IV. System Identification

Design and analysis of the ASC requires a model of how the command u affects fan power. However, dynamics of HVAC systems are highly uncertain, so modeling from first principles is likely to be inaccurate. In this section, we describe how an input-output model was fit to data obtained at our test bed.

It is known that a physics-based model for HVAC system dynamics is nonlinear. For the purposes of control, it is found that a linear input–output model can be fit to data within the frequency range of interest. The input of the system is the actuation command u, while the output is the power deviation from its baseline power profile, i.e., δP. Since we consider two different inputs, u_1 and u_2, we will identify two input-output models: u_1 to δP, which we will call H_1, and u_2 to δP, which we will call H_2.

A. Sine-Sweep Experiments

Frequency domain identification is preferable to fitting a parameterized linear model because of strict constraints on the magnitude of the inputs. Due to the large measurement noise, the sine-sweep method was used for estimating the frequency response [22].

Sine-sweep tests were conducted by modifying the fan speed (or mass flow rate setpoint) command through the control software in such a way that u_1 (u_2) becomes a sinusoidal signal with given frequency. In these experiments, the nominal fan power was equal to 2.5 kW, and for each frequency, the number of data points collected was approximately 500.

We describe first the identification of the transfer function from u_1 to δP, denoted by H_1. The frequency response estimates obtained from the experiment are shown in Fig. 8. The magnitude plot peaks between the frequency $f \in [1/(1 \text{ min}),\ 1/(30 \text{ s})]$. For lower frequency, the input is rejected by the local controller; for higher frequency, the response decays due to the dynamics of the fan and motor. A "best-fit" linear model obtained from this experiment has second-order transfer function

$$\hat{H}_1(s) = \frac{0.0173s + 1.7280 \times 10^{-6}}{s^2 + 0.0360s + 0.0144}. \quad (1)$$

Its frequency response is shown on the left-hand side of Fig. 8.

Similarly, sine-sweep experiments using input u_2 were conducted to obtain frequency response data used for identifying the system from u_2 to δP, denoted by H_2. The fitted transfer function is

$$\hat{H}_2(s) = \frac{1.809 \times 10^{-5}}{s^2 + 0.04455s + 0.01205}. \quad (2)$$

The results of these experiments are summarized in the plots shown in Fig. 8. The frequency response shows that the system has a nearly constant gain in the range $f \in [1/(10 \text{ min}),\ 1/(1 \text{ min})]$, which simplifies control design to track reference in this frequency range.

V. Controller Design and Simulation

The details of the controller design and simulation study are summarized in this section.

Recall the discussion in Section II-B: large variation in the fan speed or air flow rate is to be avoided. Such variations are undesirable also due to the possibility of equipment damage and violation of indoor air quality standards [19]. In addition, the fan speed command is subject to magnitude constraints, since it takes values between 0 and 100%.

For these reasons, the frequency ranges for providing ancillary service are chosen where the system has large gain. Considering the frequency response identified in Section IV leads to $f \in [1/(1 \text{ min}),\ 1/(30 \text{ s})]$ for ASHFS and $f \in [1/(10 \text{ min}),\ 1/(1 \text{ min})]$ for ASLAF. The controllers are designed to ensure closed loop stability and close-to-unity gain of the closed-loop frequency response in their respective frequency bands of operation.

We do not attempt to track reference signals of frequency lower than 1/(10 min). The reason is that if the fan speed or air flow rate is increased or reduced for long time periods, power consumption at the chiller will be affected; while variations in fan speed or air flow rate at higher frequency ranges will be “filtered out” by the low-pass characteristics of the chiller, and hence do not impact power consumption at the chiller [15].

A. ASHFS

The band of frequencies in which the controller is required to perform reference tracking is narrow, $f \in [1/(1 \text{ min}),\ 1/(30 \text{ s})]$, and the passband of the transfer function H_1 is very narrow. Hence, a proportional controller was found to be adequate for ASHFS. The proportional gain k_p was tuned so that: 1) $H_1^{ry}(j\omega)$ is close to one in the frequencies of interest for good tracking performance and 2) $|H_1^{ry}(j\omega)|$ is small outside that range for noise and disturbance rejection. The proportional gain $k_p = 15$ meets these criteria.

The variation in fan speed has to be limited as discussed earlier. We took the maximum allowed fan speed variation to be 10% of its nominal value, somewhat conservatively, since variations higher than 10% are sometimes observed during normal operations. The nominal power consumption of the fan motor was 2.5 kW (rated capacity = 15 kW), and we assumed somewhat arbitrarily that using more than 40% of the nominal power for ancillary services will be too aggressive. The peak magnitude of the reference signal to be tracked is therefore taken to be 1 kW. To avoid actuator saturation, we therefore need $|H_1^{ru}(j\omega)| \leq 0.1 = -20\,\text{dB}$ in the range where frequency regulation will be provided. This constraint is also satisfied by the controller.

B. ASLAF

A lag compensator was chosen $C_{\text{lag}}(s) = k(s - z/s - p)$, in which $z > p$. With the pole set to $p = -0.0017$, the zero set to $z = -0.6283$, and gain set to $k = 30$, it was found that good tracking performance was obtained with small actuation.

The frequency response of the closed-loop system, $H_2^{ry}(s)$, which is not shown due to lack of space, has nearly unit gain in the frequency range of interest, $f \in [1/(10 \text{ min}),\ 1/(1 \text{ min})]$, indicating that good tracking should be achieved in that range.

It was assumed that the maximum supply air flow rate variation allowed is 1000 CFM of its nominal value, and the reference signal to be tracked has a peak magnitude of 1 kW. This is equivalent to $|H_2^{ru}(j\omega)| \leq 60\,\text{dB}$, which is also met in the frequency range of interest.

C. Reference Signals and Bandpass Filters

Three distinct reference signals (δP_r) are used in the simulations and experiments in this paper. Two of them are obtained from the ACE signal as δP_{BA}; in particular, ACE data from PJM on 05/04/2009. A tenth-order Butterworth filter was used to obtain δP_r. The passbands of the corresponding bandpass filters are chosen to be $f \in [1/(1 \text{ min}),\ 1/(30 \text{ s})]$ for ASHFS and $f \in [1/(10 \text{ min}),\ 1/(1 \text{ min})]$ for ASLAF. In each case, the passband gain is chosen so that the peak amplitude of δP_r is approximately 1 kW. In the sequel, we will call the first δP_r the fast ACE, and the second, slow ACE. The third reference signal is RegD, which is broadcast by PJM to frequency regulation participants. In this case, the bandpass filter is simply a gain of 1 kW.

D. Performance Criteria

The dual goals of the ASC are frequency regulation to the grid, while maintaining indoor climate quality as well as low cost to the building operator. Metrics to quantify performance are described here.

1) Ancillary Service: A natural metric to quantify the quality of tracking error $e(i) := \delta P_r(i) - \delta\hat{P}(i)$ is the ratio $r_R = (\sqrt{1/N \sum_{i=1}^{N} e(i)^2}/\max|\delta P_r(t)|)$. We also evaluate the ASC using PJMs performance score S_t, based on the formula given in their manual [17]. The total performance score S_t is the mean of three scores: correlation score S_c, delay score S_d, and precision score S_p. A score of $S_t \geq 0.75$ is required to qualify to take part in PJMs ancillary service market.

2) Indoor Climate: Indoor climate quality is quantified using the temperature violation D_T defined in [23]. This score is zero if the temperature is between 70 °F and 75 °F and

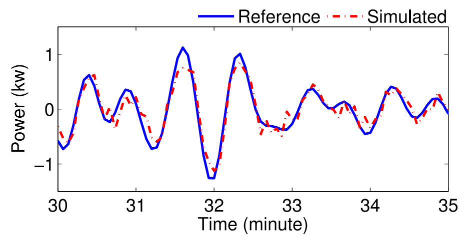

Fig. 9. Simulation result of ASHFS: 5-min slice of the data.

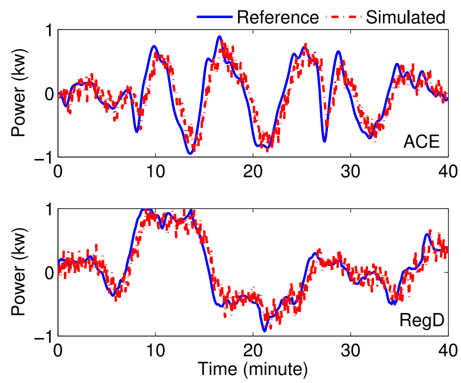

Fig. 10. Simulation result of ASLAF. Top: slow ACE as reference signal. Bottom: RegD as reference signal.

score increases if the temperature deviates from these bounds. These bounds are chosen according to the thermal comfort specifications described in [24, Ch. 8].

Variation in supply air flow rate is quantified by

$$\delta\bar{m} = \frac{\sum_{i=1}^{N}\left|\frac{m(i)-m_b(i)}{m_b(i)}\right|}{N}, \delta m_x = \max_i \left|\frac{m(i)-m_b(i)}{m_b(i)}\right| \quad (3)$$

where m is the measured supply air flow rate and m_b is the baseline supply air flow rate. Large variation in airflow rate is undesirable, as discussed in Section II-B.

E. Simulation Results

Prior to testing on an actual building, simulations were conducted using the identified models $\hat{H}_1$ and $\hat{H}_2$. Based on the discussion in Section III, measurement noise was simulated with iid zero-mean Gaussian random variables with $\sigma = 0.1$.

The ASHFS was tested using the fast ACE signal, and the ASLAF was tested with slow ACE and RegD. The reference signals and the resulting power deviations are shown in Figs. 9 and 10. The resulting performance metrics are shown in Table I. The PJM performance score S_t are above the required threshold 0.75 in all experiments. In simulations, the true power deviation without the measurement noise is also available. The performance metrics recalculated with the true values are also shown in Table I.

VI. Experimental Results

Each experiment was conducted over a 40 min time duration using the AHU2 of Pugh Hall. Forty minutes is equal to the length of the test required by PJM to meet their qualification criteria [17]. Findings from experiments surveyed here were consistent with simulation experiments, though performance sometimes degraded slightly in building tests.

TABLE I
Performance Metrics in Simulation

Simulation	Reference	S_t	r_R
ASHFS	Fast ACE	0.86	0.18
ASHFS (True output)	Fast ACE	0.89	0.15
ASLAF	Slow ACE	0.79	0.25
ASLAF (True output)	Slow ACE	0.82	0.22
ASLAF	RegD	0.85	0.18
ASLAF (True output)	RegD	0.88	0.15

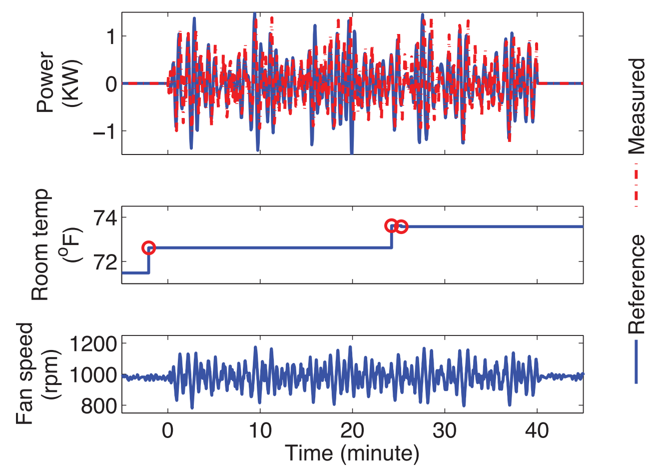

Fig. 11. Experimental results with the ASHFS controller in Pugh Hall.

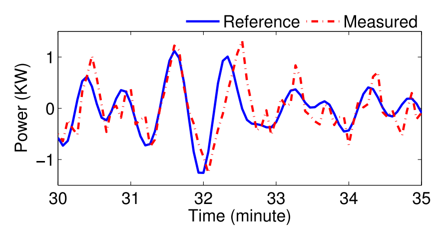

Fig. 12. Five-minute slice of the data from the ASHFS experiment.

Commands from the ASC were executed by modifying the commands from the building's existing climate control system, as described in Section III.

We observed from historical Pugh Hall data that under the existing building climate control system, the frequency of fan power variation is lower than 1/(30 min). Thus, in all closed-loop control experiments, the high-pass filter to obtain the power deviation from the baseline was chosen as a first-order Butterworth with cutoff frequency at 1/(30 min). The component in the power measurements with lower frequencies than the cut-off frequency is the baseline from the existing building climate control system.

A. ASHFS Experiments

To test the ASHFS, we use the fast ACE signal described in Section V-E. The tracking performance, room temperature variation, and supply air flow rate during the test are shown in Fig. 11. A five-minute closeup of tracking performance is also shown in Fig. 12.

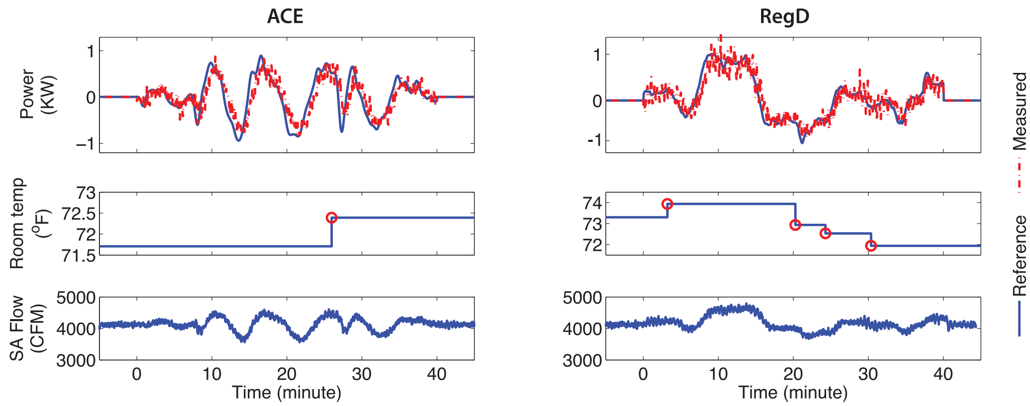

Fig. 13. Experimental results for ASLAF with lag compensator. Left: with filtered ACE as reference signal. Right: with RegD as reference signal.

TABLE II
PERFORMANCE METRICS FOR EXPERIMENTS

Test	Reference	r_R	PJM performance score			
			S_c	S_d	S_p	S_t
ASHFS	Fast ACE	0.30	0.80	1	0.41	0.74
ASLAF	Slow ACE	0.27	0.94	0.94	0.44	0.77
ASLAF	RegD	0.19	0.94	0.95	0.60	0.83

TABLE III
EFFECTS OF ASC ON ROOM CLIMATE

Test	Reference	D_T	$\delta\bar{m}$ (%)	δm_x (%)
ASHFS	Fast ACE	0	3.4	17.1
ASLAF	Slow ACE	0	3.4	13.8
ASLAF	RegD	0	3.9	15.0

The PJM score 0.74 taken from Table II is marginally lower than the threshold 0.75. This score is lower than that in the simulation. The mismatch might be caused by the poor fit of the model $\hat{H}_1$—based on which the controller is designed—and the experimentally determined frequency response.

The variation in room temperature is small, with $D_T = 0$. The variation in supply air flow rate can be calculated by subtracting the estimated baseline value from the measured data. As shown in Table III, the average variation is less than 4% and the maximum variation is less than 20%.

B. ASLAF Experiments

The experimental setup again followed the setup for the simulations described in Section V-E, with the slow ACE and RegD signals as reference and the lag compensator to compute the control command. Data from two typical runs are shown in Fig. 13. Despite noise and uncertainties in the real building, the experimental data showed good tracking and very good match with the simulation results. The control system's scores summarized in Table II exceeded PJMs threshold for both the reference signals. Table III shows that the effect on room climate is negligible, and the airflow rate variation is small.

C. Reducing Effect of Noise in Performance Estimation

The PJM scores might be better than reported above since measurement noise in P–which affects $\delta\hat{P}$–is included in the computation, though the service provided depends only on the actual power deviation, not its noisy measurement.

TABLE IV
PERFORMANCE METRICS WITH FILTERED MEASUREMENTS

Test	Reference	r_R	PJM performance score			
			S_c	S_d	S_p	S_t
ASHFS	Fast ACE	0.27	0.83	1	0.49	0.77
ASLAF	Slow ACE	0.24	0.98	0.94	0.50	0.81
ASLAF	RegD	0.14	0.99	0.94	0.73	0.89

To improve the estimate of power deviation we passed the measurements through a bi-directional low-pass filter. The filter used is a fifth-order Butterworth filter with cutoff frequency at $1/(30\ \mathrm{s})$ for ASHFS experiments and $1/(60\ \mathrm{s})$ for ASLAF experiments. Recalculated with this filtered power deviation, performance scores improved; see Table IV. In particular, all of them exceed PJMs 0.75 requirement.

D. Economic Potential

What is the economic value of Pugh Hall or similar buildings to a BA? An estimate of the revenue that can be obtained from PJM can be computed based on their publicly available policy manuals [25], [26].

The AHU2 fan provided 1 kW capacity of frequency regulation during its operational hours, during which time its nominal power consumption is 2.5 kW. There are two other AHUs which normally operates at 7 and 5 kW. Assuming that all 3 AHUs provide the same ratio of their nominal power for ancillary services as AHU2 does, which is 40% (1 kW/2.5 kW), all the AHU fans in Pugh Hall can provide $0.4(2.5 + 7 + 5) = 5.8$ kW capacity for frequency regulation. Assuming that Pugh Hall provides 5.8 kW of capacity of RegD service during each of its operational hours (6 A.M.–11 P.M.), the yearly revenue for the building is estimated to be \$1421 based on PJMs market data for 2013 [27]. The total maximum capacity of the AHU fans in Pugh Hall is 75 kW, so the revenue will increase if the fans operate at higher power.

VII. CONCLUSION

This paper demonstrates through experiments that fan motors in commercial building HVAC systems can provide frequency regulation service to the power grid without impacting indoor climate. In fact, the experiments with filtered

ACE demonstrate that loads may be used for faster services than frequency regulation, since the frequencies of the filtered ACE signal was higher than that of the fastest reference signal provided by PJM, RegD. Although there is currently no demand for tracking such high-frequency regulation signals, there is motivation to consider tracking problems that are more demanding than PJMs RegD. For instance, if loads are used in primary control or for voltage control, faster dynamic response may be required.

Experimental results show that the system passes the qualifying tests to participate in PJMs frequency regulation service market. This 40 000 sq. ft. building would generate approximately \$1400 revenue per year based on PJMs 2013 prices.

In the experiments reported here, the air flow rate is varied either directly by commanding the fan speed or indirectly by commanding the flow rate setpoint. In HVAC systems where the air flow rate is controlled through static pressure setpoint, control can be executed by varying the static pressure setpoint.

Large measurement noise from the VFD and uncertain communication delay in control execution are potential hurdles to higher controller performance. Improvement in hardware to provide power measurements with higher accuracy and resolution, and improvement in software to reduce delay in command execution, are likely to improve performance.

It is not known if the variations in fan speed that result from providing ancillary services can lead to degradation to motors or other equipment over long time periods. This is a potential risk of this technology, and needs to be thoroughly studied.

There are many directions for future research. There are many other loads in a building, such as chillers and pumps, which can also be used to provide ancillary service without affecting their quality of service [15]. Alternatives to the information architecture assumed here should be considered. For example, it may be useful to take control actions based on local frequency deviations in the power lines along with a global signal broadcast from the BA.

Acknowledgment

The authors would like to thank personnel at the Physical Plants Division at the University of Florida, in particular P. Winkel, for their help in conducting the field tests in Pugh Hall.

References

[1] S. Meyn, M. Negrete-Pincetic, G. Wang, A. Kowli, and E. Shafieepoorfard, "The value of volatile resources in electricity markets," in *Proc. 49th IEEE Conf. Decis. Control (CDC)*, Atlanta, GA, USA, Dec. 2010, pp. 1029–1036.

[2] B. Kirby. (2007). *Ancillary Services: Technical and Commercial Insights*. [Online]. Available: http://tinyurl.com/kax2ek4

[3] Federal Energy Regulatory Commission, *Order No. 755 Frequency Regulation Compensation in the Wholesale Power Markets*, May 2011. [Online]. Available: http://tinyurl.com/oba9oow

[4] D. Lew, G. Brinkman, E. Ibanez, B. Hodge, and J. King, "The western wind and solar integration study phase 2," Nat. Renew. Energy Lab., Golden, CO, USA, Tech. Rep. NREL/TP-5500-55588, 2013.

[5] N. Lu, "An evaluation of the HVAC load potential for providing load balancing service," *IEEE Trans. Smart Grid*, vol. 3, no. 3, pp. 1263–1270, Mar. 2012.

[6] J. MacDonald, P. Cappers, D. Callaway, and S. Kiliccote, "Demand response providing ancillary services," presented at the Grid-Interop, Irving, TX, USA, Dec. 2012. [Online]. Available: http://tinyurl.com/k3pqmdp

[7] H. Hao, T. Middelkoop, P. Barooah, and S. Meyn, "How demand response from commercial buildings will provide the regulation needs of the grid," in *Proc. 50th Annu. Allerton Conf. Commun. Cont. Comput.*, Monticello, IL, USA, Oct. 2012, pp. 1908–1913.

[8] U.S. Department of Energy. (2011). *Buildings Energy Data Book.* [Online]. Available: http://buildingsdatabook.eren.doe.gov/

[9] J. L. Mathieu, "Modeling, analysis, and control of demand response resources," Ph.D. dissertation, Dept. Mech. Eng., Univ. Calif., Berkeley, CA, USA, 2012.

[10] N. Lu and Y. Zhang, "Design considerations of a centralized load controller using thermostatically controlled appliances for continuous regulation reserves," *IEEE Trans. Smart Grid*, vol. 4, no. 2, pp. 914–921, Jun. 2013.

[11] B. Biegel *et al.*, "Aggregation and control of flexible consumers—A real life demonstration," in *Proc. 19th IFAC World Congr.*, Cape Town, South Africa, May 2014, pp. 1–6.

[12] S. Meyn, P. Barooah, A. Busic, and J. Ehren, "Ancillary service to the grid from deferrable loads: The case for intelligent pool pumps in Florida," in *Proc. 52nd IEEE Conf. Decis. Control*, Florence, Italy, Dec. 2013, pp. 6946–6953.

[13] D. Todd *et al.*, "Providing reliability services through demand response: A preliminary evaluation of the demand response capabilities of Alcoa Inc.," *Oak Ridge Nat. Lab.*, Oak Ridge, TN, USA, vol. 233, Jan. 2008.

[14] H. Hao, A. Kowli, Y. Lin, P. Barooah, and S. Meyn, "Ancillary service for the grid via control of commercial building HVAC systems," in *Proc. Am. Control Conf. (ACC)*, Washington, DC, USA, Jun. 2013, pp. 467–472.

[15] Y. Lin, P. Barooah, and S. P. Meyn, "Low-frequency power-grid ancillary services from commercial building HVAC systems," in *Proc. IEEE Int. Conf. Smart Grid Commun. (SmartGridComm)*, Vancouver, BC, Canada, Oct. 2013, pp. 169–174.

[16] H. Hao, A. Kowli, Y. Lin, P. Barooah, and S. Meyn, "Ancillary service to the grid through control of fans in commercial building HVAC systems," *IEEE Trans. Smart Grid*, vol. 5, no. 4, pp. 2066–2074, Jul. 2014.

[17] *PJM Manual 12: Balancing Operations, Rev. 27*, PJM, Audubon, PA, USA, Dec. 2012.

[18] "Commercial buildings energy consumption survey (CBECS): Overview of commercial buildings," Energy Information Administration, Department of Energy, U.S. Govt., 2003. [Online]. Available: http://tinyurl.com/pw6nsjy

[19] *American Society of Heating, Refrigerating and Air Conditioning Engineers*, ASHRAE Standard 62.1, 2004.

[20] C. Hubner, T. Hansemann, and H. Merz, *Building Automation*, ser. Signals and Communication Technology. Berlin, Germany: Springer, 2009, pp. 185–273.

[21] T. Middelkoop, "High-resolution data collection for automated fault diagnostics," in *Automated Diagnostics and Analytics for Buildings*, B. L. Capehart and M. Brambley, Eds., Atlanta, GA, USA: Fairmont Press, 2014, pp. 271–290.

[22] L. Ljung, *System Identification: Theory for the User*, 2nd ed. Englewood Cliffs, NJ, USA: Prentice Hall, 1999.

[23] S. Goyal, H. Ingley, and P. Barooah, "Occupancy-based zone climate control for energy efficient buildings: Complexity versus performance," *Appl. Energy*, vol. 106, pp. 209–221, Jun. 2013.

[24] ASHRAE, *The ASHRAE Handbook Fundamentals (SI Edition)*. Atlanta, GA, USA: Amer. Soc. Heat. Refrigerating Air Conditioning Eng., 2005.

[25] *PJM Manual 28: Operating Agreement Accounting*, Rev. 62, PJM, Audubon, PA, USA, Aug. 2012.

[26] *PJM Manual 11: Energy and Ancillary Services Market Operations*, Rev. 62, PJM, Audubon, PA, USA, Dec. 2013.

[27] PJM. (2014). *PJM Regulation Zone Preliminary Billing Data.* [Online]. Available: http://www.pjm.com/markets-and-operations/market-settlements.aspx

Authors' photographs and biographies not available at the time of publication.